GEOPHYSICAL RESEARCH LETTERS, VOL. 17, NO. 6, PAGES 889-892, MAY 1990

MARTIAN BOW SHOCK: PHOBOS OBSERVATIONS

K. Schwingenschuh, W. Riedler and H. Lichtenegger

Space Research Institute

Ye. Yeroshenko

IZMIRAN

K. Sauer

Institut fur Kosmosforschung

J. G. Luhmann, M. Ong and C. T. Russell

Institute of Geophysics and Planetary Physics

Abstract. Data obtained with the MAGMA magnetometer on the subsolar passes of the Phobos spacecraft during its 3 elliptic orbits reveals a turbulent bow shock with a strong foot consistent with the reflection of solar wind protons. The bow shock lies at a subsolar distance of 1.47 $\pm$ .03 R_M. The circular orbit phase of the mission reveals a bow shock with a highly varying location. The median terminator crossing lies at 2.72 Mars radii. The location of the bow shock in the terminator plane is sensitive to neither the EUV flux nor to planetary longitude.

Introduction

Bow shocks form to deflect the supersonic solar wind around any sufficiently large obstacle to the flow. The existence of a bow shock says very little about the nature of the obstacle, only that an obstacle exists. The obstacle might be formed by a planetary magnetosphere, such as at the Earth; by a planetary ionosphere, such as at Venus; or by mass addition to the flow, such as at comets. The structure, the location and shape of the bow shock are affected by the nature of the interaction. Obviously, the stronger a planetary magnetic field the further away the solar wind is deflected by the planet and the further out the bow shock stands. At comets the same principle holds. The greater the mass loading of the solar wind, which in turn is proportional to the outgassing rate of the comet, the greater is the stand off distance of the shock. The shape of the bow shock is also affected by the nature of the interaction. A body that has a substantially greater radius at the flanks than at the subsolar point will have a bow shock that flares more than a shock in front of a spherical object. A magnetosphere has such an out-of-round shape. The shape in the plane perpendicular to the solar wind may also be asymmetric. For example the magnetodisk of Jupiter causes an asymmetric shock [Slavin et al., 1985]. Also asymmetric mass loading in the Venus magnetosheath is believed to cause an asymmetric bow shock [Russell et al., 1988]. Finally, the structure of the bow shock is determined in part by the nature of the interaction. At a comet, mass loading of the solar wind at great distances from the comet leads to instabilities and the growth of upstream waves far from the comet and ahead of the bow shock [Smith et al., 1986]. This mass loading also slows the flow so that the shock is weaker. The strong waves combined with the small jump in parameters across the shock due to its low Mach number leads to a rather diffuse shock in front of the comets.

While aspects of the Martian bow shock have been studied for over 2 decades since the Mariner 4 data were acquired [Greenstadt, 1970] the Phobos mission allowed the bow shock of Mars to be probed at high temporal resolution for the first time. Magnetic field measurements with a resolution of 1.5 seconds were obtained on three passes through the subsolar bow shock [Riedler et al., 1989]. Moreover approximately 50 passes through the Martian wake were obtained with a temporal resolution of 45 sec in the circular orbit phase at close to the orbit to Phobos. Figure 1 shows the initial elliptical orbit and a circular orbit in the equatorial plane of Mars together with the trace of the bow shock rotated into a common plane assuming asymmetry about the Sun-Mars line. The effective size of the obstacle to the solar wind is also shown as deduced using the gas dynamic model of the interaction [Riedler et al., 1989]. We see that the initial orbit moves almost tangentially to the subsolar bow shock, thus providing good spatial resolution of

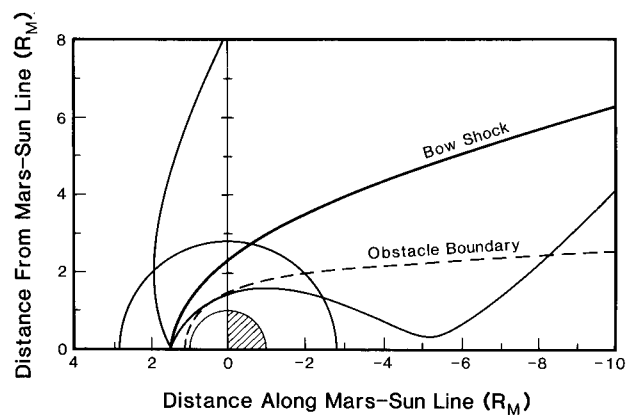

Fig. 1. The orbit of the Phobos spacecraft during the elliptical and circular orbit phases mapped in the plane containing the Sun-Mars line and the spacecraft. The bow shock and inferred obstacle boundary are shown [Riedler et al., 1989].

Paper number 90GL00521
0094-8276/90/90GL-00521$03.00

the region. The circular orbit phase provides repeated coverage of the shock near the terminator but the lower temporal resolution (45-sec) during this phase provides correspondingly less information on the temporal and spatial structure of the shock in this region. It is the purpose of this paper to examine first the structure and location of the subsolar shock as seen on the first three elliptical orbits and then to examine the location of the bow shock as observed during the circular orbit phase. Other papers discuss the upstream wave region [Russell, 1990] and the apparently induced magnetotail [Yeroshenko et al., 1990].

The Subsolar Bow Shock

The magnetic field magnitude as observed as the spacecraft crossed the bow shock on the first three elliptical orbits is shown in Figure 2. The three crossings are remarkably similar. The magnetic field is initially about 2.7 nT on each day and then approximately doubles over a period of about 15 minutes to a value of about 6 nT. Then it jumps to about 12 nT. Through this region the fluctuation amplitude grows as the main shock jump is approached. Strong fluctuations are seen downstream from the shock as well as upstream.

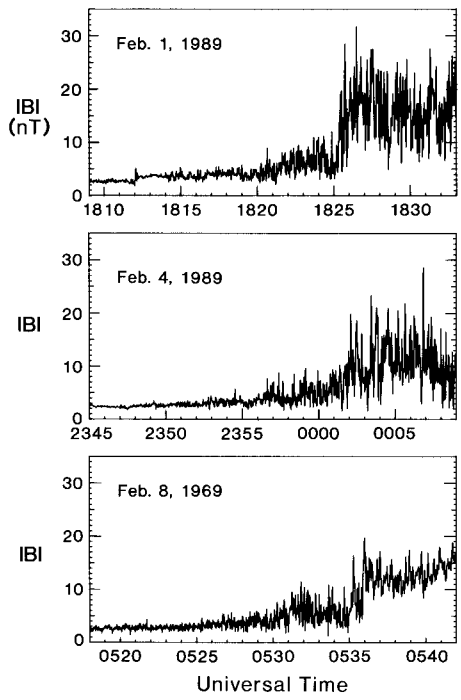

Fig. 2. The magnetic field strength at 1.5 sec resolution across the three subsolar bow shock encounters.

Figures 3 and 4 show power spectra of the trace of the spectral matrix of the fluctuations seen for 10-minute intervals just before the shock and just after the shock. The power level just ahead of the shock is about 1 order of magnitude greater than in the undisturbed IMF far upstream [cf. Russell et al., 1990]. At low frequencies the power level increases another order of magnitude in crossing the shock. However on February 8, the power at high frequencies drops in crossing the shock.

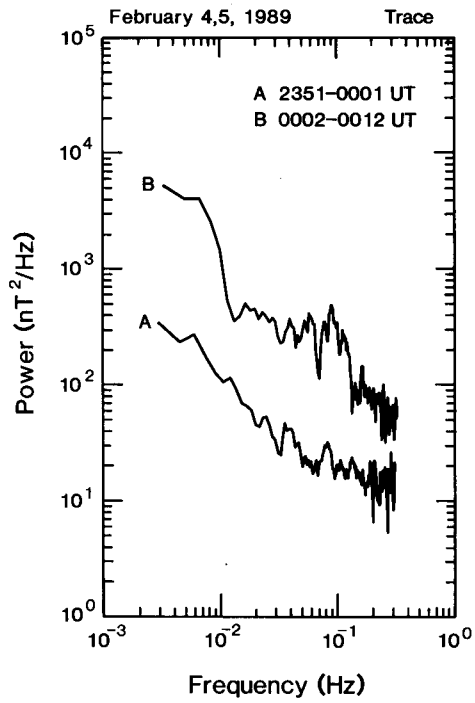

Fig. 3. Power spectra of the trace of the spectral matrix a) in the foot of the shock and b) post-shock on February 4, 5.

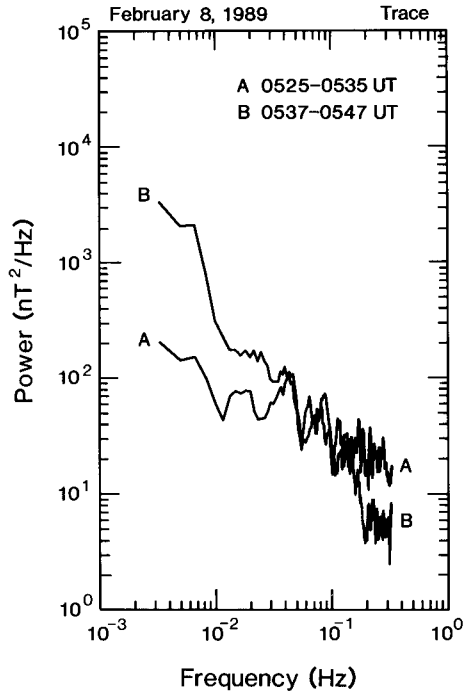

Fig. 4. Power spectra of the trace of the spectral matrix a) in the foot of the shock and b) post-shock on February 8.

The rise in field magnitude is seen more clearly in Figure 5 in which the data have been filtered with a low pass filter with a corner frequency of 0.01 Hz. The location of each of these shocks is given in Mars Solar Orbital coordinates (MSO) for the midpoint of the magnitude rise in Table 1.

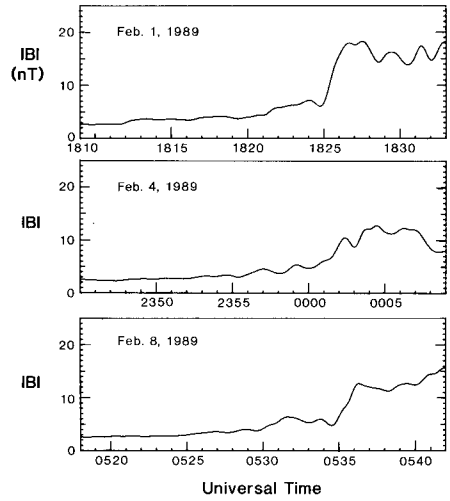

Fig. 5. The magnetic field strength on the first three orbits low pass filtered with a 0.01 Hz corner frequency.

Extrapolating these positions to the aberrated subsolar point using the shock shape and average aberration angle to be derived below we find that the average subsolar shock position on these three days was 1.47 Mars radii (R_M) with a probable error of the mean of 0.03 R_M. This number in terms of Venus radii is identical to the subsolar radius of the Venus bow shock at solar maximum [Zhang et al., 1990]. Also given in Table 1 is the angle between the model shock normal and upstream field for each of these shocks. They are all quasi-perpendicular shocks.

The rise in magnitude of the field seen ahead of the bow shock appears to be the foot of the bow shock associated with reflected ions [cf. Gosling and Thomsen, 1985]. The most obvious onset of this foot is on February 1 at 1812 UT when the spacecraft was at (1.79, -.43, 0.36) R_M in aberrated MSO coordinates. Extrapolating from the bow shock location observed later on this day and using the shape of the bow shock deduced below the bow shock radius at this solar zenith angle was 1.48 R_M. Thus the foot of the shock was 1350 km thick at this time. If the solar wind were flowing at its median value of 440 km/s at this time, the foot should have a minimum thickness of 1150 km [Gosling and Thomsen, 1985]. On February 4 and 8 the IMF magnitude was similar to that on February 1, although slightly different in direction. Thus, assuming no change in solar wind conditions the size of the foot should be similar on all 3 days. Figure 5 shows this to be the case. As pointed out by Moses et al. [1988] such a large reflected ion gyro radius means that the downstream magnetosheath plasma will not have room to thermalize before flowing by the planet. This may account for some of the turbulence seen downstream in Figure 2.

The Shape of the Shock

The shape of the obstacle to the solar wind affects the shape of the resulting bow shock. We can determine the shape of the bow shock by combining our determination of the location of the subsolar shock on the elliptic orbits with a determination of the location of the bow shock on the circular orbits. These latter crossings occur near the terminator plane. Figure 6 shows the X-component of the location of the bow shock crossing in MSO coordinates on each of the circular orbits for the dawn and dusk crossings separately. The histogram running through the center of each panel shows the 4-day running median of the shock location shifted every 2 days. The difference in the average location of the dawn and dusk bow shock crossings is equivalent to an aberration angle of 3.8° or an average solar wind velocity of 365 km/sec during the circular orbit phase.

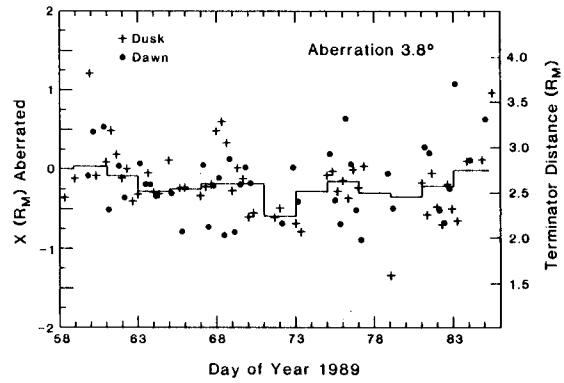

Fig. 6. The X-location in MSO coordinates with X-toward the sun of the bow shock crossing corrected for an average aberration angle of 3.8°. The right-hand scale gives the equivalent terminator location of the shock assuming a fixed eccentricity of 0.85. The histogram is a running 4-day median shifted every 2 days.

Using the average subsolar shock location of 1.47 R_M and the average 3.8° aberration angle we can find the terminator shock location which best fits the data in Figure 6. We obtain a distance of 2.72 R_M with an eccentricity of 0.85 for a conic with the planet at the focus. This compares with the value of 2.40 R_V for the terminator shock location at Venus during the maximum of solar activity in 1979 [Russell et al., 1988]. The terminator distances of 2.52 and 2.91 R_M enclose 50% of the bow shock encounters. A similar analysis for Venus during solar maximum yields terminator shock distances of 2.26 and 2.53 R_V. Thus, not only is the Mars shock relatively further from the planet at the terminators but also it is somewhat more variable in location. The distance between the quartiles, 0.39 R_M, is 14% of the

Table 1. Subsolar Bow Shock Locations

Orbit	Time	Location (MSO Coord)	Distance	SZA	R_{ss}	Theta Bn
1	Feb. 1, 1825:20	(1.44, 0.21, 0.00) R_M	1.46 R_M	8.4°	1.45	88°
2	Feb. 5, 0001:45	(1.44, 0.18, 0.00)	1.45	7.0°	1.44	56°
3	Feb. 8, 0535:30	(1.52, -.01, 0.06)	1.52	2.5°	1.52	57°

SZA - solar zenith angle; R_{ss} - subsolar radius in Mars radii; Theta B_n - angle between IMF and model shock normal.

terminator radius at Mars as compared to 11% at Venus.

The location of the bow shock appears to be quite variable. This variability may be due to such solar wind variations as changes in the flow direction of the solar wind, Mach number, the cone angle between the magnetic field and the flow, and the clock angle in the Y-Z plane between the shock encounter and the field direction and/or variations in the EUV flux [Russell et al., 1988]. It is not possible at the present stage of data reduction to examine each of these possibilities. However, we have examined the F10.7 cm solar flux as proxy for the EUV flux and find no significant correlation between shock location and F 10.7 cm flux taking into account the difference between Earth and Mars in solar longitude. The variability could also be due to some geographically fixed enhancement in ionospheric pressure such as could be provided by a strongly magnetized surface region. Such magnetized regions, present on the surface of the moon, cause deflection of the solar wind as it passes the lunar terminator [cf. Russell and Lichtenstein, 1975]. To cause the observed variability of the Martian shock these regions would have to be significantly more strongly magnetized than on the Moon. We have plotted the bow shock locations versus planetary longitude for both dawn and dusk encounters and see no control by planetary longitude. Hence the variable shock position does not seem to be caused by any intrinsic planetary magnetic field.

Conclusions

The subsolar Mars bow shock as deduced from 3 subsolar passes of the Phobos spacecraft lies at $1.47 \pm .03\ R_M$. The shock has a foot in which the magnetic field doubles prior to the shock ramp. The size of this foot is about 1350 km or somewhat under one gyro radii of a specularly reflected solar wind proton. This distance is also roughly the thickness of the Martian magnetosheath. Both the foot and the magnetosheath are quite turbulent.

The circular orbits provide many crossings of the shock in the near terminator region. These data reveal a shock with a quite variable shock location with a ratio of terminator to nose location of 1.85 compared to 1.66 for Venus [Zhang et al., 1990] and a median location of $2.72\ R_M$. This greater distance than observed at Venus could be caused by relatively greater mass loading at Mars than at Venus or by planetary magnetism perhaps localized. This distance is also greater than those deduced from the elliptic phase alone [Riedler et al., 1989] and from earlier missions [Vaisberg et al., 1990]. These differences may reflect temporal variations in the interaction and differences in shock shape with distance from the planet. The simple formula we have used here may not be applicable much beyond the terminator region.

The variability of the terminator shock location seems much greater than that at the nose but this apparent constancy at the nose may be more apparent than real because of the paucity of data here, only 3 crossings. Nevertheless, there are more sources of terminator shock location variability than that for the nose. Mach number changes that affect shock shape and size and solar wind directional variability will affect the terminator more than the nose. This is a feature we also have difficulty addressing at Venus.

Acknowledgments. We would like to thank the many people on the Phobos project who made these measurements possible. The work at UCLA was supported by the National Aeronautics and Space Administration under grant NGW-1753.

References

Gosling J. T. and M. F. Thomsen, Specularly reflected ions, shock foot thicknesses, and shock velocity determinations in space, J. Geophys. Res., 90, 9893-9896, 1985.

Greenstadt, E. W., Dependence of shock structure at Venus and Mars on orientation of the interplanetary magnetic field, Cosmic Electrodynamics, 1, 380-388, 1970.

Moses, S. L., F. V. Coroniti and F. L. Scarf, Expectations for the microphysics of the Mars-solar wind interation, Geophys. Res. Lett., 15, 429-432, 1988.

Riedler, W. et al., Magnetic fields near Mars: First results of the Phobos mission, Nature, 341, 604-607, 1989.

Russell, C. T. and B. R. Lichtenstein, On the source of lunar limb compressions, J. Geophys. Res., 80, 4747-4750, 1975.

Russell, C. T., E. Chou, J. G. Luhmann, P. Gazis, L. H. Brace and W. R. Hoegy, Solar and interplanetary control of the location of the Venus bow shock, J. Geophys. Res., 93, 5461-5469, 1988.

Russell, C. T., J. G. Luhmann, K. Schwingenschuh, W. Riedler and Ye. Yeroshenko, Upstream waves at Mars: Phobos observations, Geophys. Res. Lett., in press, 1990.

Slavin, J. A., E. J. Smith, J. R. Spreiter and S. S. Stahara, Solar wind flow about the outer planets: Gas dynamic modeling of the Jupiter and Saturn bow shocks, J. Geophys. Res., 90, 6275-6286, 1985.

Smith, E. J., B. T. Tsurutani, J. A. Slavin, D. E. Jones, G. L. Siscoe and D. A. Mendis, International Cometary Explorer encounter with Giacobini-Zinner: Magnetic field observations, Science, 232, 382-385, 1986.

Vaisberg, O. L., J. G. Luhmann and C. T. Russell, Plasma observations of the solar wind interaction with Mars, J. Geophys. Res, 95, in press, 1990.

Yeroshenko, Ye., W. Riedler, K. Schwingenschuh, J. G. Luhmann, M. Ong and C. T. Russell, The magnetotail of Mars: Phobos observations, Geophys. Res. Lett., in press, 1990.

Zhang, T. L., J. G. Luhmann and C. T. Russell, Solar cycle dependence of the location and shape of the Venus bow shock, J. Geophys. Res., 95, in press, 1990.

K. Schwingenschuh, W. Riedler and H. Licthenegger, Space Reserch Institute, Graz, Austria.

Ye. Yeroshenko, IZMIRAN, Toritsk, Moscow Region, USSR.

K. Sauer, Institut fur Kosmosforschung, 1194 Berlin, Rudower Chausse 5, GDR.

J. G. Luhmann, M. Ong and C.T. Russell, Institute of Geophysics and Planetary Physics, University of California, Los Angeles, CA 90024-1567.

(Received November 20, 1989;
revised January 29, 1990;
accepted February 19, 1990)